



ELSEVIER

Available online at www.sciencedirect.com

ScienceDirect

www.elsevier.com/locate/jes

JES

JOURNAL OF
ENVIRONMENTAL
SCIENCESwww.jesc.ac.cn

Research article

Electrochemically assisted production of biogenic palladium nanoparticles for the catalytic removal of micropollutants in wastewater treatment plants effluent[☆]

Q2

Cindy Ka Y Law^{a,b}, Kankana Kundu^{a,b}, Luiza Bonin^{a,b},
Lorena Peñacoba-Antona^{c,d}, Eduardo Bolea-Fernandez^e, Frank Vanhaecke^e,
Korneel Rabaey^{a,b}, Abraham Esteve-Núñez^{c,d,f}, Bart De Gussemé^{a,b},
Nico Boon^{a,b,*}

^a Center for Microbial Ecology and Technology (CMET), Ghent University, Coupure Links 653, B-9000 Gent, Belgium

^b Centre for Advanced Process Technology for Urban Resource recovery (CAPTURE), P.O. Frieda Saeystraat 1, B-9000 Gent, Belgium

^c METfilter S.L., Autovía A49 Sevilla-Huelva Km 28, 41820 Carrión de los Céspedes, Sevilla, Spain

^d IMDEA Water Institute, Av. Punto Com, 2, Parque Científico Tecnológico, 28805 Alcalá de Henares, Madrid, Spain

^e Atomic & Mass Spectrometry (A&MS) research group, Department of Chemistry, Ghent University, Campus Sterre, Krijgslaan 281-S12, B-9000 Ghent, Belgium

^f Universidad de Alcalá, Department of Analytical Chemistry, Physical Chemistry and Chemical Engineering, Ctra. Madrid-Barcelona Km 33.600, 28871 Alcalá de Henares, Madrid, Spain

ARTICLE INFO

Article history:

Received 30 June 2022

Revised 11 August 2022

Accepted 11 August 2022

Available online xxx

Keywords:

Antibiotics

Adsorption

Biogenic palladium nanoparticles

Catalytic activity

H₂

Secondary treated municipal wastewater

ABSTRACT

Biogenic palladium nanoparticles (bio-Pd NPs) are used for the reductive transformation and/or dehalogenation of persistent micropollutants. In this work, H₂ (electron donor) was produced *in situ* by an electrochemical cell, permitting steered production of differently sized bio-Pd NPs. The catalytic activity was first assessed by the degradation of methyl orange. The NPs showing the highest catalytic activity were selected for the removal of micropollutants from secondary treated municipal wastewater.

The synthesis at different H₂ flow rates (0.310 L/hr or 0.646 L/hr) influenced the bio-Pd NPs size. NPs produced over 6 hr at a low H₂ flow rate had a larger size (D₅₀ = 39.0 nm) than those produced in 3 hr at a high H₂ flow rate (D₅₀ = 23.2 nm). Removal of 92.1% and 44.3% of methyl orange was obtained after 30 min for the NPs with sizes of 39.0 nm and 23.2 nm, respectively. Bio-Pd NPs of 39.0 nm were used to treat micropollutants present in secondary treated municipal wastewater at concentrations ranging from µg/L to ng/L. Effective removal of 8 compounds was observed: ibuprofen (69.5%) < sulfamethoxazole (80.6%) < naproxen (81.4%) < furosemide (89.7%) < citalopram (91.7%) < diclofenac (91.9%) < atorvastatin (>

Q2

[☆] Webpage: cmet.Ugent.be

* Corresponding author at: Ghent University; Faculty of Bioscience Engineering; Center for Microbial Ecology and Technology (CMET); Coupure Links 653; B-9000 Gent, Belgium

E-mail: Nico.Boon@UGent.be (N. Boon).

<https://doi.org/10.1016/j.jes.2022.08.018>

1001-0742/© 2022 The Research Center for Eco-Environmental Sciences, Chinese Academy of Sciences. Published by Elsevier B.V. This is an open access article under the CC BY-NC-ND license (<http://creativecommons.org/licenses/by-nc-nd/4.0/>)

Please cite this article as: Cindy Ka Y Law, Kankana Kundu, Luiza Bonin et al., Electrochemically assisted production of biogenic palladium nanoparticles for the catalytic removal of micropollutants in wastewater treatment plants effluent, Journal of Environmental Sciences, <https://doi.org/10.1016/j.jes.2022.08.018>

94.3%) < lorazepam (97.2%). Removal of fluorinated antibiotics occurred at > 90% efficiency. Overall, these data indicate that the size, and thus the catalytic activity of the NPs can be steered and that the removal of challenging micropollutants at environmentally relevant concentrations can be achieved through the use of bio-Pd NPs.

© 2022 The Research Center for Eco-Environmental Sciences, Chinese Academy of Sciences. Published by Elsevier B.V.

This is an open access article under the CC BY-NC-ND license (<http://creativecommons.org/licenses/by-nc-nd/4.0/>)

Introduction

1 Anthropogenic activities are rapidly exacerbating environ-
2 mental pollution (Gautam et al., 2019). Pharmaceuticals and
3 various chemical compounds of environmental concern are
4 present in many products used daily. These products are a
5 significant source of pollution, reaching a broadening area
6 through the effect of greater urbanization worldwide. Al-
7 though effective removal of macropollutants is achieved
8 through traditional wastewater treatment plants (WWTP),
9 this is not the case for micropollutants. Micropollutants such
10 as antibiotics, personal care products, detergents, and dyes,
11 are rarely controlled before the discharge of the wastewater
12 into the environment, as their removal at low concentrations
13 lacks effectiveness (de Andrade et al., 2018, Jiang et al., 2020,
14 Pandey et al., 2020). The presence of micropollutants in the
15 environment is undesirable due to their impact on the ecosys-
16 tem and human health (Pandey et al., 2020). One of the emerg-
17 ing micropollutants is antibiotics, which are mainly used to
18 cure diseases in humans and animals (Cao et al., 2017). The
19 presence of this in the environment has severe adverse conse-
20 quences on their effectiveness for curing diseases due to the
21 development of (multi-) resistant bacteria and genes (Cao et
22 al., 2017, Liu et al., 2019, Jiang et al., 2020). Dyes are also used
23 broadly in the industry for, e.g., cosmetics, pharmaceuticals,
24 paper, and agricultural compounds (Khataee and Kasiri, 2010).
25 They have been associated with mutagenic and carcinogenic
26 repercussions for human health (Pandey et al., 2020). There-
27 fore, it is important to remove these micropollutants effec-
28 tively and avoid their discharge into the environment.

29 Common techniques for the removal of antibiotics and
30 dyes are adsorption, membrane filtration, and advanced ox-
31 idation processes (AOP) (Abtahi et al., 2018, de Andrade et al.,
32 2018, Pandey et al., 2020). Adsorption and membrane filtration
33 are only temporary solutions in which, the micropollutants
34 are transferred away from the wastewater rather than being
35 treated (degradation in metabolites), while the wastestream
36 also contains a high ionic load (cations and anions) (Bobu et
37 al., 2013, Yagub et al., 2014). The disadvantages of AOP are the
38 high energy consumption and costs, as well as the production
39 of secondary toxic wastestreams (Abtahi et al., 2018, Anjali
40 and Shanthakumar, 2019). Therefore, it is essential to find
41 an environmentally friendly and highly efficient method that
42 does not produce toxic and high concentrated wastestreams
43 alongside the removal of antibiotics and dyes. The use of bio-
44 genic palladium nanoparticles (bio-Pd NPs) for the removal
45 of pharmaceutical compounds and dyes has been tested with
46 promising results (Forrez et al., 2011, Wang et al., 2018). How-

ever, the application of bio-Pd NPs for the removal of fluori-
nated pharmaceutical compounds (e.g., ciprofloxacin, citalo-
pram, and atorvastatin), which are highly used and for which
removal efficiencies tend to be low, have not been well stud-
ied yet (Forrez et al., 2011, Miao et al., 2018, Osawa et al., 2019,
Antonelli et al., 2020). Martins et al. (2016), assessed the re-
moval of several antibiotics by bio-Pd NPs, but no removal of
fluorinated antibiotics as a result of the catalytic activity of
the NPs was detected. The study was carried out in a synthetic
medium, where the matrix composition is fairly simple in con-
trast to real environmental matrices (Martins et al., 2017). Nev-
ertheless, a removal of 87.7% of ciprofloxacin was found after
25 hr and at pH = 3.2 with 30 mg of Pd in the form of bio-Pd
NPs (He et al., 2020). The disadvantage of this method is the
low pH and high concentrations of Pd needed. Moreover, the
degradation of persistent fluorinated antibiotics, other than
ciprofloxacin, with bio-Pd NPs required further study, espe-
cially in environmentally relevant matrices. Ideally, effective
removal is accomplished with the use of a lower concentra-
tion of Pd, shorter reaction time, higher pH, and in environ-
mentally relevant concentrations are required.

Bio-Pd NPs have been thoroughly studied for the removal
of various chlorinated compounds (De Corte et al., 2012, De
Gusseme et al., 2012, Hazarika et al., 2017, He et al., 2020).
Synthesis is often accomplished by the microorganisms *She-
wanella oneidensis* due to its metal-reducing properties (Lovley,
1993, Dundas et al., 2018). The formation of bio-Pd NPs also re-
quires the addition of an electron donor such as H₂, which is
the most suitable electron donor for *S. oneidensis*, due to their
intrinsic metabolism (Yang et al., 2020). Three mechanisms oc-
cur in the formation of bio-Pd NPs, (1) biological conversion
from Pd²⁺ to Pd⁰ by microorganisms, (2) chemical conversion
of palladium with H₂, and (3) autocatalytic conversion of pal-
ladium (Yang et al., 2020). The latter two processes result in
the formation of large nanoparticle clusters due to the aggre-
gation of the NPs (Deplanche et al., 2014). Large NPs is not de-
sired because of its low surface/volume ratio, whereas the cat-
alytic activity depends on the size of the bio-Pd NPs (Saldan
al., 2015). Current research targets the production of smaller
bio-Pd NPs. De Windt et al. (2006) and Hou et al. (2017) studied
the influence of cell viability by employing different Pd:Cell
Dry Weight (CDW) ratios. Nevertheless, Pd:CDW ratios along-
side other production parameters can be tested over virtually
unlimited ranges (De Windt et al., 2006, Hou et al., 2017). The
production of bimetallic bio-Pd NPs has also been extensively
studied, with the second metal often being catalytically active
as well (Tuo et al., 2017, Gomez-Bolivar et al., 2019, Omajali et
al., 2019, Sivamaruthi et al., 2019). In this way, the catalytic ac-
tivity of the bio-Pd NPs can be increased by the second metal,

Q3

96 resulting in a higher removal efficiency of the micropollutants
97 (Omajali et al., 2019). The disadvantage of this method is that
98 the addition of a second metal increased the costs and that ad-
99 ditional steps are needed before and after production. It is also
100 possible to enhance the catalytic activity by reshaping the mi-
101 croorganisms and attached palladium nanoparticles through
102 the use of an activation agent such as potassium hydroxide
103 (KOH) (Xiong et al., 2018). Although the catalytic activity in-
104 creases, the conditions to obtain the change in morphology
105 are stringent and expensive to maintain. Therefore, finding a
106 more feasible method to control or steer the production of the
107 bio-Pd NPs size is a high priority.

108 In this work, the production of different sized bio-Pd NPs
109 was controlled by: (1) adsorption of Pd²⁺ on *Shewanella onei-*
110 *densis* (biosorption) before the exposure to the electron donor
111 H₂ (0 hr, 24 hr, and 48 hr), (2) low (0.310 L/hr) and high (0.646
112 L/hr) H₂ concentrations in the liquid phase, and (3) the contact
113 time (3 hr or 6 hr) between H₂, Pd²⁺, and *Shewanella oneiden-*
114 *sis*. H₂ was produced by an electrochemical cell (EC) to control
115 the availability of H₂, and thus, to steer the size of bio-Pd NPs.
116 When bio-Pd NPs are produced, an electron donor is required
117 to reduce Pd²⁺ to Pd⁰ microbially (Yang et al., 2020), therefore,
118 the concentration of electron donor was never controlled by
119 an electrochemical system before. Here, H₂, electrochemically
120 produced, will be used by the microbial cells to convert the
121 palladium, but will also be used for chemical and autocatalytic
122 conversion of Pd²⁺ to Pd⁰. The catalytic activity of the different
123 bio-Pd NPs was first tested using methyl orange. Based on the
124 results obtained for the removal of methyl orange, the bio-Pd
125 NPs with the highest removal efficiency was selected and used
126 for the removal of a mixture of micropollutants (including flu-
127 orinated antibiotics) present in the secondary treated munic-
128 ipal wastewater. Here, 25 different compounds were detected,
129 of which 8 compounds are discussed in detail.

1. Materials and methods

1.1. Chemicals

131 The Na₂PdCl₄ powder (98%), phosphate-buffered saline (PBS)
132 tablets, Luria Bertani (LB) used for bio-Pd NPs production, and
133 methyl orange for the activity test were purchased from Merck
134 (Merck, Germany). M9 medium used for washing the bio-Pd
135 NPs was prepared based on the recipe provided by Merck and
136 contained KH₂PO₄, Na₂HPO₄, NaCl and NH₄Cl purchased from
137 Carl Roth (Carl Roth, Germany). KOH tablets used as electrolyte
138 was purchased from Carl Roth. For ICP-MS analysis, ultra-pure
139 water (resistivity > 18.2 MΩ cm, Millipore, France). Pro anal-
140 ysis purity level 14 mol/L HNO₃ (ChemLab, Belgium), further
141 purified by sub-boiling distillation, and 9.8 mol/L H₂O₂ (Fluka,
142 Belgium) were used for acid digestion. 1 g/L single-element
143 standard solutions of Pd and Rh (Instrument Solutions, The
144 Netherlands) were used for method development and calibra-
145 tion purposes, and for internal standardization, respectively.

1.2. Bio-Pd NPs solution preparation

147 The production of bio-Pd NPs was carried out as described by
148 De Windt et al. (2005). *Shewanella oneidensis* MR-1 cells were

grown in LB medium overnight at 28°C on a shaker (New 149
Brunswick Scientific, Belgium) and harvested by centrifuging 150
at 10,000 g for 10 min. The cells were washed three times with 151
M9 medium and resuspended in M9 medium to a final opti- 152
cal of OD₆₁₀ = 0.5 with Spectronic 200 (Thermofischer, USA). 153
Na₂PdCl₄ was added to the resuspended solution at a concen- 154
tration of 50 mg/L Pd²⁺; this solution was incubated overnight 155
on a shaker at 20°C (Appendix A Table S1.). Production of dif- 156
ferent types of bio-Pd NPs (Appendix A Table S1.) was per- 157
formed in a custom-built experimental setup (Fig. 1). Corre- 158
sponding controls were prepared in the same manner but 159
were not exposed to H₂. The bio-Pd NPs produced and con- 160
trols were washed three times with PBS and stored at 5°C. 161

1.3. Experimental setup for bio-Pd NPs production

A custom-built experimental setup (in triplicate) containing 163
an EC connected to a glass column was used to produce bio- 164
Pd NPs. A two-compartment EC (dimensions: 23.5 × 9.0 × 2.5 165
cm) made from two Perspex® frames was used to separate the 166
cation exchange membrane (CEM) (Membrane International 167
Inc., USA) from the electrodes. A stainless-steel electrode was 168
used as the cathode (dimensions: 5 × 20 cm) and an iridium 169
electrode was used as the anode. Between the compartments 170
and CEM, rubber sheets were placed to create a liquid-tight 171
seal, and the frames were bolstered. A pump at a flow rate 172
of 252 mL/min (Watson Marlow NV, Belgium), was used to re- 173
circulate the KOH electrolyte. The current of the EC was con- 174
trolled by a power supply (Velleman, Belgium), Faraday's Law 175
was used to calculate the amount of H₂ produced based on 176
the current applied. The EC was connected to a glass column 177
(wrapped in aluminum foil to prevent light penetration), in 178
which the microorganisms/Pd²⁺ solution was transferred in, 179
after incubation. The top of the glass column was connected 180
to a gascounter. The bottom of the column contained a two- 181
way connector between the EC and a gasbag for N₂ flushing, 182
both regulated by a valve. 183

1.4. Bulk ICP-MS analysis and TEM images

Bulk ICP-MS, Agilent 8800 ICP-MS instrument (Agilent Tech- 185
nologies, Japan), analysis was performed to determine the 186
concentration of Pd in the different bio-Pd NP samples. TEM 187
JEOL JEM 1010 (Jeol, Japan) images were taken to confirm the 188
particle size. The D50 particle size was determined by ImageJ 189
software. 190

For bulk analysis, the bio-Pd samples were acid digested 191
in closed Savillex® PFA beakers prior to ICP-MS. 5 mL of sus- 192
pended bio-Pd in PBS was centrifuged at 10,000 g for 30 min, 193
after which the supernatant was removed. The resulting pellet 194
was acid digested with 1.5 mL of 14 mol/L HNO₃ and 0.5 mL 195
of 9.8 mol/L H₂O₂. The closed beakers were heated to 115°C 196
overnight on a hot plate. After complete mineralization, the 197
digestates were evaporated at 90°C until dryness, then redis- 198
solved in 2.0 mL of 0.35 mol/L HNO₃. This solution was further 199
diluted with 0.35 mol/L HNO₃ and Rh was added as the inter- 200
nal standard (final concentration = 2 µg/L) to compensate for 201
potential matrix effects and/or signal instability. 202

For TEM analysis, 1.0 mL suspended bio-Pd in PBS was cen- 203
trifuged at 5000 g for 5 min and washed three times with 1.0 204

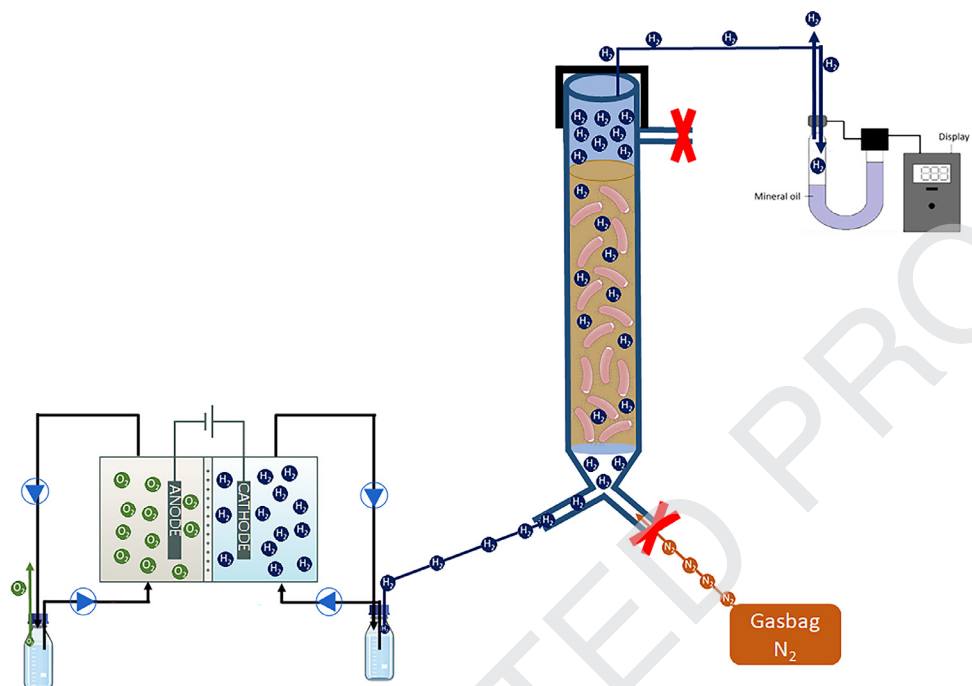


Fig. 1 – Experimental setup for a steered bio-Pd NPs production through the use of an EC.

205 mL ultra-pure water (Millipore, France). Subsequently resus-
 206 pended in 1.0 mL of ultra-pure water. 2.0 μL of the solution was
 207 placed on the formvar-coated Cu single slot grid (Agar, UK),
 208 dried for 20 min at 37°C spent overnight in the Jeol EM-DSC20
 209 vacuum chamber (Jeol, Japan). TEM images were taken with
 210 a Jeol JEM 1010 TEM at 60 kV, equipped with a side-mounted
 211 charge coupled device (CCD) Veleta camera (EMSIS GmbH, Ger-
 212 many).

213 1.5. Catalytic activity test with methyl orange

214 The catalytic activity of bio-Pd NPs was evaluated by the re-
 215 moval of 100 mg/L methyl orange (in biological triplicates), in
 216 serum flasks. Suspended bio-Pd was centrifuged at 10,000 g
 217 for 10 min, and the pellet of centrifuged bio-Pd corresponded
 218 to 80.95 μg Pd. The pellet was resuspended in 19.2 mL of dis-
 219 tilled water and 0.8 mL of methyl orange stock solution (7.63
 220 mmol/L) was added. The serum flasks were flushed with 100%
 221 N_2 for 20 cycles, subsequently, 120 mL of 100% H_2 was added.
 222 1 mL sample was taken at 0, 10, 15, 30, 50, 70, 90, 110, and 120
 223 min and was filtered using a 0.20 μm filter. The absorbance
 224 was measured at a $\lambda_{\text{max}} = 465$ nm using a Spectronic 200 (Ther-
 225 moFischer, USA). Distilled water and (filtered) suspended bio-
 226 Pd in distilled water were used as a control for the absorbance
 227 measurements. Suspended microorganisms without Pd were
 228 used as a control for the catalytic activity test.

229 1.6. Removal of emerging compounds from secondary 230 treated municipal wastewater

231 Removal of micropollutants in secondary treated wastewa-
 232 ter (in duplicate) was tested with the bio-Pd NPs showing the
 233 highest activity, as selected based on the results of section

234 2.5. The raw wastewater first went through primary treat- 234
 235 ment, whereafter the effluent went to secondary treatment, 235
 236 described elsewhere (Peñacobá-Antona et al., 2021). A sample 236
 237 of this secondary treated wastewater was taken, represent- 237
 238 ing $t_0 = 0$ min. The removal of the micropollutants present in 238
 239 the secondary effluent was performed with centrifuged 9.41 239
 240 mg Pd, resuspended the pellet in 700 mL of secondary efflu- 240
 241 ent in 1 L Schott bottles. The Schott bottles were wrapped in 241
 242 aluminum foil and flushed with 100% N_2 for 20 cycles, where- 242
 243 after 240 mL of H_2 (100%) was immediately added and another 243
 244 240 mL of H_2 (100%) was added 1 hr later and was placed on a 244
 245 stirrer. Samples were taken at 2 hr and 24 hr and were cen- 245
 246 trifuged at 10,000 g for 10 min. The supernatants were filtered 246
 247 through a 0.20 μm filter. Secondary effluent with only H_2 and 247
 248 autoclaved *Shewanella oneidensis* with H_2 were used as controls 248
 249 for the test. 249

250 1.7. Detection of the emerging compounds

251 The micropollutants were extracted with a multi-residue 251
 252 method (solid-phase extraction) from the treated secondary 252
 253 effluent and were detected with LC-MS/MS, described in detail 253
 254 elsewhere (de Santiago-Martín et al., 2020). An aliquot (100 mL) 254
 255 of the sample was passed through an Oasis HLB cartridge (200 255
 256 mg, 6 cc, Waters, USA) and eluted with methanol. Two chro- 256
 257 matographic separations were necessary. In positive ioniza- 257
 258 tion mode, the Kinetex Biphenyl column (50 \times 3 mm, 2.7 μm , 258
 259 Phenomenex, Torrance, CA, USA) was used. The mobile phases 259
 260 were 0.1% (v/v) formic acid in ultrapure water (phase A) and 260
 261 0.1% (v/v) formic acid in MeOH (phase B). Compounds in nega- 261
 262 tive ionization mode were separated using the Poroshell 120 262
 263 EC-C18 column (50 \times 3 mm, 2.7 μm , Agilent Technologies). The 263
 264 mobile phases used were 5 mmol/L ammonium fluoride in ul- 264

trapure water (phase A) and MeOH:MeCN (65.35, v/v) (phase B). For both separations, the flow rate of the mobile phase was 0.6 mL/min, and the sample injection volume of 20 μ L.

2. Results and discussion

2.1. Small nanoparticles are formed with high continuous availability of H₂

The influence of (1) the adsorption (biosorption) of Pd²⁺ on *Shewanella oneidensis*, (2) the contact time between H₂, Pd²⁺, and the microorganisms, as well as (3) the flow rate of H₂ (thus the availability of H₂ in the liquid phase) on the production of bio-Pd NPs was studied (Appendix A Table S1.). Large nanoparticles (D50 = 140.0 nm, condition 1) were obtained when no adsorption of Pd²⁺ on the microorganisms took place, while smaller nanoparticles (< 100 nm) were obtained for all conditions with adsorption before the exposure to H₂. When comparing the controls, it was observed that adsorption was present between the incubated and non-incubated cells and that NPs were present in cells that were exposed to H₂. Adsorption on the cell surface was observed by TEM images, when comparing incubated and non-incubated cells, furthermore, this has also been found by other researchers (Xu et al., 2018). ICP-MS data of the controls (Appendix A Fig. S1.) also showed a difference in Pd conversion efficiency between the cells incubated for 24 hr and 48 hr. Together, with the TEM images, it can be confirmed that adsorption was present. ICP-MS data of the controls showed that there was a maximum Pd conversion efficiency of 11.7%, while in the presence of H₂ the conversion of Pd was minimal 26.9%. Hence it can be stated that with the presence of H₂ the synthesis of bio-Pd NPs is responsible for the majority of Pd conversion, but *Shewanella oneidensis* is also able to convert Pd alone as shown before in the literature (Yang et al., 2020). Nevertheless, adsorption has a strong influence on the particle size. In this work, it was hypothesized that smaller NPs would be produced when the adsorption time was longer as this causes higher adsorption of Pd²⁺ and subsequently higher biological conversion. However, the opposite behavior was observed here – larger nanoparticles were produced with a longer adsorption time (condition 6). The long adsorption time (48 hr) possibly inactivated the microorganisms, a hypothesis supported by the observations made by He et al. (2020), and Chen and Chen (2021). Maximal adsorption was reported by *E. coli* after 2 hr when all the sorption sites on the microorganisms were occupied by Pd²⁺ causing saturation (He et al., 2020). When high concentrations of Pd²⁺ are present in the microorganisms, this destroys the activity of the reactive oxygen scavenging enzymes. This results in high amounts of reactive oxygen species (ROS), causing bacterial damage and ultimately death, as found for *Bacillus wiedmannii* (Chen and Chen, 2021). Production of small bio-Pd NPs in the biosorption process was also observed (Xu et al., 2018). The produced bio-Pd NPs can autocatalytically convert the attached Pd²⁺ on the already formed bio-Pd NPs, with the longer reaction time contributing to the higher autocatalytic conversion and resulting in larger NPs.

When comparing condition 2 (23.2 nm) and 3 (53.2 nm) in which, bio-Pd NPs are produced at a high flow rate of H₂ (0.646

L/hr H₂), it was observed that larger NPs were obtained when the contact time between H₂, Pd²⁺, and the microorganisms was longer (6 hr). In contrast, smaller NPs, condition 5 (39.0 nm) compared to 4 (75.6 nm), were obtained when a lower flow rate (0.310 L/hr H₂) and a longer exposure time with H₂ (6 hr) were used. Hence, contradictory data were obtained for the two exposure times and H₂ flow rates. This is because the exposure time depends on the H₂ flow rate, thus the availability of H₂ in the liquid phase, which is confirmed when comparing condition 2 with 5, and 3 with 4. The availability of H₂ produced during 6 hr with 0.310 L/hr is equal to that produced during 3 hr with 0.646 L/hr. The use of a longer exposure time and a higher H₂ flow rate results in a higher degree of chemical and autocatalytic conversion, and hence, agglomeration as a result of which larger nanoparticles are produced. Nevertheless, a long exposure time is required with a low H₂ flow rate to have sufficient H₂ for the biological conversion of Pd²⁺. Different conversions from Pd²⁺ to Pd⁰ were found when different formate concentrations were tested, with the highest reductions (99%) of Pd²⁺ when a 25-fold higher formate concentration was used (Yang et al., 2020). However, different observations were found in this work. The greater solubility of formate over H₂ leads to its preferential uptake in solution. Therefore, the *in situ* production of H₂ is necessary to steer the size of the nanoparticles during bio-Pd NPs synthesis.

2.2. The size of the nanoparticles is independent of the conversion efficiency of Pd²⁺ to Pd⁰

The conversion efficiency of Pd²⁺ into bio-Pd NPs was determined through ICP-MS, which allowed the determination of the average mass of Pd in and around the cells (Fig. 2A). High conversion efficiencies were observed for condition 1 (50.1 \pm 6.8%) and 6 (44.8 \pm 7.4%), which corresponds to a D50 nanoparticle size of 140.0 nm and 62.8 nm respectively. Strong chemical and autocatalytic conversion were present for condition 1 and 6, which was confirmed by the TEM images (Fig. 2B). The size of the latter conditions was 2-fold larger, while the difference in conversion efficiency between condition 1 and 6 was only 5.3%. The differences in size and conversion efficiency between the two conditions do not vary in a linear way, which is due to the prior adsorption of Pd²⁺ for 48 hr. The adsorption of Pd²⁺ on the microorganisms is responsible for 11.7% (Appendix A Fig. S1) of the conversion efficiency. When this adsorption is not taken into consideration, then only 33.1% of the conversion efficiency originated from the nanoparticles formed, which is similar for condition 2, 3, 4, and 5. Hence, this confirms that the adsorption time of 48 hr caused the production of large NPs (see section 3.1).

Similar conversion efficiencies could be seen for condition 2, 3, 4 and 5, i.e. 31.8 \pm 1.4 %, 33.8 \pm 2.0 %, 30.2 \pm 5.3% and 26.9 \pm 5.2% respectively. This corresponded to a D50 particle size of 23.2 nm, 53.2 nm, 75.6 nm, and 39.0 nm respectively. While the variation in size is large, the difference in conversion efficiency is low based on the controls the influence of the adsorption of Pd²⁺ on *Shewanella oneidensis* before the exposure of H₂ can be considered negligible (Appendix A Fig. S1). This can be explained by the number of nanoparticles present around the cells, when condition 2 and 5 are compared, the difference in size is 3-fold while this is not the case for the conversion

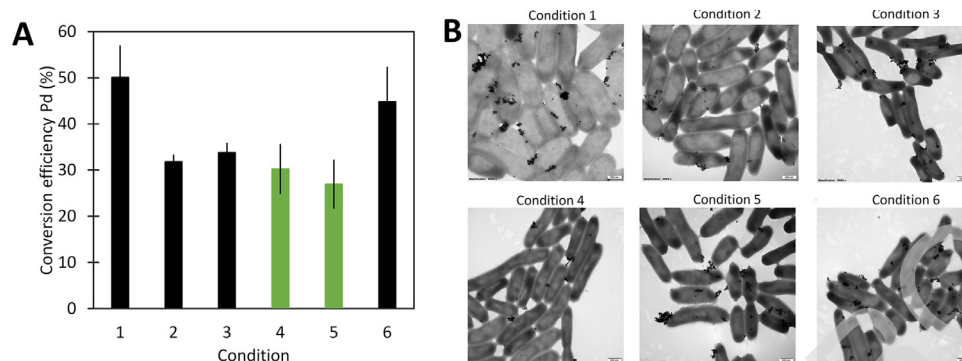


Fig. 2 – A: The conversion efficiency of Pd into bio-Pd NPs as determined by ICP-MS. The different conditions are indicated on the x-axis and the conversion efficiency of Pd on the y-axis. B: The corresponding TEM images of the different types of bio-Pd NPs.

378 efficiency. The difference is not caused by the adsorption, as
 379 for both conditions, the amount of Pd²⁺ adsorbed is similar.
 380 Consequently, the difference is likely caused by the distribu-
 381 tion and hence the number of nanoparticles around the cells.
 382 When small nanoparticles are formed, it was observed that
 383 a high number of nanoparticles are present. The absence of
 384 agglomeration indicates that mainly biological conversion is
 385 present. The high number of small nanoparticles under con-
 386 dition 2 compared to 4 can be seen in the TEM images (Fig. 2B).
 387 Furthermore, it can be concluded that the increase in the size
 388 of nanoparticles corresponds with a decrease in the number
 389 of nanoparticles. This statement was concise with the find-
 390 ing of De Windt et al. (2006), where it was observed that a low
 391 number of nanoparticles were found when the nanoparticle
 392 size was large.

393 2.3. The highest catalytic activity for the removal of 394 methyl orange was not obtained with the smallest NPs

395 The catalytic activity of the different bio-Pd NPs (80.95 µg Pd
 396 was used) was tested through the degradation of 100 mg/L
 397 methyl orange (Fig. 3), by measuring the decolorization at
 398 λ_{max} = 465 nm. Once methyl orange is decolorized, it was as-
 399 sumed that this compound was degraded into intermediates.
 400 It was proposed by Nguyen et al. (2018), in which Pd doped
 401 TiO₂ was used for photocatalysis, such that the N–C and azo
 402 bonds (-N=N-) were specifically targeted (Nguyen et al., 2018).
 403

404 High removal of methyl orange was demonstrated for all
 405 different types of bio-Pd NPs, except for condition 1. This
 406 is due to the large size of the nanoparticles, resulting in a
 407 low surface/volume ratio, and hence low catalytic activity (De
 408 Windt et al., 2006). Complete degradation was found after 120
 409 min for condition 3, 4, and 5, with condition 5 showing the
 410 highest removal efficiency, the D50 nanoparticles' sizes were
 411 53.2 nm, 75.6 nm, and 39.0 nm respectively. The removal effi-
 412 ciencies found for these three conditions were: 99.0 ± 0.8%,
 413 99.5 ± 0.4%, and 99.7 ± 0.2% respectively. It was expected
 414 that condition 2 with the smallest nanoparticles would con-
 415 tribute to the highest catalytic activity of the bio-Pd NPs (De
 416 Windt et al., 2006, Rotaru et al., 2012, Saldan et al., 2015). How-
 417 ever, the catalytic activities from high to low for the differ-
 418 ent conditions were 5 > 4 > 3 > 6 > 2, which corresponds to

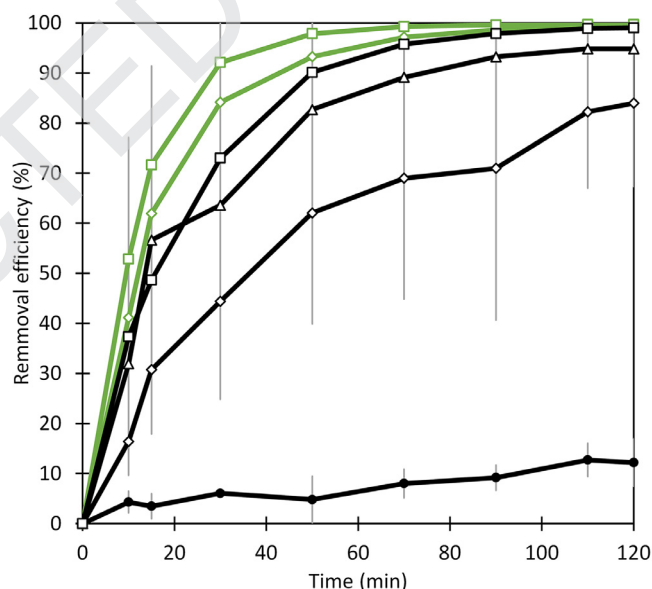


Fig. 3 – The catalytic activity of the different bio-Pd NPs (80.95 µg Pd) as tested using 100 mg/L of methyl orange. The time is plotted on the x-axis and the removal efficiency for methyl orange on the y-axis. Removal efficiency of bio-Pd NPs produced according to condition 1 (●), condition 2 (⊙), condition 3 (□), condition 4 (◇), condition 5 (▲) and condition 6 (△).

418 NPs sizes of 39.0 nm > 75.6 nm > 53.2 nm > 62.8 nm > 23.2
 419 nm, respectively. While the difference in size is not large, be-
 420 tween condition 2 and 5, the difference in activity rather is.
 421 The high activity of condition 5, where 99.7 ± 0.2% removal
 422 efficiency was established within 120 min can be explained
 423 by the small size of the Pd NPs spread over the microorgan-
 424 ism, which is following the findings by De Windt et al. (2006).
 425 The low removal of the bio-Pd NPs of condition 2 (84.0% ±
 426 16.7% in 120 min), was not expected. However, besides the
 427 size, the catalytic activity of the NPs is also affected by de-
 428 fects, and modifications of the metal by light elements, e.g. ox-
 429 idation, and dissolution of hydrogen and/or carbon (Yudanov
 430 et al., 2011). It is possible that the higher number of small
 431

431 NPs present on the cells in condition 2, caused the disintegration of the microbial cells, resulting in the release of carbon, 432 and thereby influencing the catalytic activity. Furthermore, it 433 was found by Yudanov et al. (2011), that structures of truncated octahedron, which exhibits bulk-like face-centered cubic 434 are the most stable, while non-crystallographic packings, 435 like icosahedron- or decahedron-based shapes shows competition 436 in between small clusters of metal clusters. The density 437 function showed that icosahedral structures are energetically 438 preferred over the face cubic center-based cuboctahedral 439 structures (Yudanov et al., 2011). However, within the octahedron 440 structure, different metal clusters are present, resulting in 441 different adsorption positions, found for CO bindings 442 (Yudanov et al., 2003). Therefore, it is possible that condition 443 2 had less favorable clustering of the metal particles, causing 444 a lower catalytic activity. Condition 3 had higher activity than 445 6 due to the smaller size of NPs. However, the high activity of 446 condition 4 was not anticipated, hence all the bio-Pd NPs produced 447 at a lower H₂ flow rate showed better catalytic activity. 448 It was found that the activity is independent of the NPs for 449 a size range between, 2.5 – 6.6 nm (Ershov et al., 2014). However, 450 this is not the case here, as the size difference in the NPs 451 is larger. The following hypothesis is made for the high catalytic 452 activity of bio-Pd NPs formed under condition 4. During 453 the 3 hr production of bio-Pd NPs, the formed nanoparticles 454 possibly adsorbed the H₂ present in the solution for bio-Pd 455 NPs production. Due to the large size of NPs, a large number 456 of H₂ molecules could be adsorbed on the surface. Therefore, 457 it is feasible that the catalytic activity and the high concentration 458 of the adsorbed H₂ on the nanoparticles resulted in a 459 higher removal of the methyl orange than with the smaller 460 nanoparticles formed under condition 3, 6, and 2. Furthermore, 461 it is also possible that condition 4 had a high number of NPs 462 distributed on the microorganisms. However, the effect of the 463 large (condition 4) and small (condition 2) nanoparticle size 464 for the high and low removal needs to be further investigated. 465 Nevertheless, compared to the literature, condition 2, 3, 4, 5, 466 and 6 had a higher removal efficiency for methyl orange 467 (Freitas et al., 2021). Freitas et al. (2021) produced chemical Pd 468 NPs with maghemite as support for the NPs. Although small 469 NPs sizes were obtained, 5 nm, decolorization of only 79% in 470 240 min was achieved, which needed 2-fold more time and 471 had lower removal efficiency than condition 2 (Freitas et al., 472 2021).

475 2.4. Removal of micropollutants in secondary treated 476 wastewater is observed by bio-Pd NPs

477 The bio-Pd NPs with the highest catalytic activity (section 3.3)
478 were selected and tested for the removal of a diverse mixture
479 of micropollutants present in the secondary treated effluent,
480 also referred as WWTP effluent in this paper. Wastewater
481 coming from a treatment plant was used because of the
482 environmentally relevant matrix and realistic concentrations
483 of the micropollutants (ng/L – µg/L). In this complex matrix,
484 25 compounds were selected to determine the removal efficiency
485 (Appendix A Table S2). However, the main focus will be on 8
486 compounds, atorvastatin, citalopram, diclofenac, furosemide,
487 ibuprofen, lorazepam, naproxen, and sulfamethoxazole (Table
488 1). These compounds were chosen due to their frequent use

and the poor investigation that has been performed on these
micropollutants.

Although low amounts of Pd (13.4 mg/L Pd wastewater) were used, high removal efficiencies for all compounds were obtained after 2 hr treatment, > 69%. From low to high, the removal efficiency was as follows: ibuprofen < sulfamethoxazole < naproxen < furosemide < citalopram < diclofenac < atorvastatin < lorazepam. The additional removal of the pollutants after 24 hr treatment was considered to be irrelevant. Removal after 24 hr was low compared to the removal established after 2 hr, due to the binding sites of the Pd-H NPs (Han et al., 2009). When high numbers of micropollutants are present, all the Pd-H NPs sites are occupied for the degradation of these pollutants. As degradation of the micropollutants proceeds, intermediates are formed, therefore it was hypothesized that a further degradation of these intermediates is possible. Consequently, with the increase in compounds to be degraded, the occupation of the Pd-H NPs is low versus the high number of pollutants, hence low removal of compounds was obtained after 24 hr.

Removal of the micropollutants is obtained through the catalytic activity of the bio-Pd NPs, which can be confirmed by the controls (Appendix A Table S2). It can be seen that neither the microorganisms present in the secondary effluent nor the inactive *Shewanella oneidensis* were able to remove the compounds by adsorption or biodegradation. Furosemide, citalopram, diclofenac, atorvastatin, and lorazepam are halogenated compounds, which showed a removal of > 90%. Bio-Pd NPs are widely used for carbon-carbon and carbon-heteroatom cross-coupling reactions, hydrogenation, and dehalogenation reactions (Hennebel et al., 2011, Adams et al., 2014). Despite that, it can be seen that the dehalogenation reaction is preferred over the other reactions (Table 1). It is hypothesized that the removal of furosemide, citalopram, diclofenac, atorvastatin, and lorazepam occurs through the dehalogenation of the halogens, i.e. chlorine, and fluorine atoms based on the chemical structure (Appendix A Fig. S2D, E, F, G, and H). Degradation of chlorinated compounds by bio-Pd NPs has been thoroughly studied and it was shown that the halogens were often released first (Quan et al., 2018). Therefore, it is assumed that dechlorination occurred for furosemide, diclofenac, and lorazepam, which resulted in removal efficiencies of 89.7 ± 2.0%, 91.9 ± 2.8%, and 97.2 ± 0.7%, respectively. However, De Gusseme et al. (2012) found complete removal of diclofenac, through dechlorination. The difference in removal is due to the complex composition of the WWTP effluent tested in this work, where a complex mixture of micropollutants was present. The Pd-H bonds on the bio-Pd NPs used for the removal of compounds were not only occupied by diclofenac but also by other micropollutants present in the wastewater, therefore, lower removal of diclofenac can be expected. The advantage of using bio-Pd NPs is that only a single by-product is formed, which decreases the production of undesired, toxic, and mutagenic intermediates (De Gusseme et al., 2012). Removal of fluorinated micropollutants was also presumed for citalopram and atorvastatin, with removal efficiencies of 91.7 ± 0.4% and > 94.3%. Removal of ciprofloxacin through the use of bio-Pd NPs was established by He et al. (2020). It was suggested that defluorination, was one of the possible degradation processes that occurred as a first step

Table 1 – Concentration and removal efficiencies of emerging compounds in treated municipal secondary wastewater, with t_0 the concentration at the start of the experiment = 0 min, t_1 the concentration of the emerging compounds at 2 hr, and t_2 the concentration of the emerging compounds after 24 hr of bio-Pd NPs treatment.

Compounds	t_0 (ng/L)	t_1 : real ww treated for 2 hr (ng/L)	t_2 : real ww treated for 24 hr (ng/L)	t_1 : Removal efficiency of treated ww (%)	t_2 : Removal efficiency of treated ww (%)
Atorvastatin	57.7	5.6	< 1.0	> 94.3	> 98.3
Citalopram	119.5	9.9 ± 0.4	< 11.8	91.7 ± 0.4	> 95.0
Diclofenac	895.0	72.1 ± 25.0	59.7 ± 31.8	91.9 ± 2.8	93.3 ± 3.6
Furosemide	1233.6	126.9 ± 24.2	96.2 ± 50.7	89.7 ± 2.0	92.2 ± 4.1
Ibuprofen	2004.5	611.7 ± 27.9	752.8 ± 347.5	69.5 ± 1.4	62.4 ± 17.3
Lorazepam	285.0	8.1 ± 1.9	5.3 ± 5.4	97.2 ± 0.7	98.1 ± 1.9
Naproxen	6893.6	1279.9 ± 463.1	929.5 ± 254.4	81.4 ± 6.7	86.5 ± 3.7
Sulfamethoxazole	521.7	101.1 ± 30.7	86.9 ± 4.5	80.6 ± 5.9	83.3 ± 0.9

(He et al., 2020). Defluorination of micropollutants is often obtained through AOP or adsorption (Alamgholiloo et al., 2021, Long et al., 2021). AOP has been extensively investigated, and therefore different types of AOP exist, however, the disadvantage of this method is that requirements need to be met before using this method. As such, catalysts are desired due to maximizing the removal potential, presence of light, and addition of iron (Chin et al., 2014, Olvera-Vargas et al., 2015, Bartolomeu et al., 2018). The use of bio-Pd NPs has more advantages demonstrated by the high removal efficiency of halogenated compounds. After dehalogenation, it is proposed that further degradation of the C=O bond, C-C bond and aromatic structures will occur through hydrogenation by bio-Pd NPs (Kluson and Cervený, 1995, Adams et al., 2014).

Besides dehalogenation, the removal of ibuprofen, sulfamethoxazole, and naproxen was also found. The controls proved that removal was obtained from the catalytic activity of bio-Pd NPs rather than from adsorption or biodegradation. It is suggested that the removal of these three compounds by bio-Pd NPs was obtained through carbon-carbon and carbon-heteroatom cross-coupling reaction (Adams et al., 2014). It is presumed that aromatic compounds will be hydrogenated afterwards (Zhang et al., 2022). Although ibuprofen and sulfamethoxazole removal were low in this study compared to the other compounds, 69.5 ± 1.4%, and 80.6 ± 5.9%, respectively, the degradation was still relatively high and fast compared to what was reported by Martins et al. (2017) and Forrez et al. (2011). Martins et al. (2017) found no removal of ibuprofen and 85% degradation of sulfamethoxazole after 24 hr of treatment with bio-Pd and bio-Pt NPs. Removal was not observed for ibuprofen partially due to the absence of adsorption (Martins et al., 2017). The degradation of ibuprofen and sulfamethoxazole with biogenic metals manganese oxide was obtained after 13 days, with concentrations decreasing from 158 to < 8 ng/L and from 259 to 256 ng/L, respectively (Forrez et al., 2011). Removal efficiencies of 81.4 ± 6.7% were obtained for naproxen in this work, which is high compared to biodegradation with *Trametes versicolor* for which 31% degradation was obtained after 24 hr (Bernats and Juhna, 2018). Biogenic metals manganese oxide was also tested by Forrez et al. (2011), but no removal was observed for naproxen after 13 days.

3. Conclusion

Steering the production of bio-Pd NPs is possible through the use of an EC for the supply of H₂ as an electron donor. In contrast to a previous hypothesis and earlier works, a lower flow rate of H₂ resulted in larger bio-Pd NPs (39.0 nm) showing higher catalytic activity, compared to the smaller NPs (23.2 nm). However, the lowest catalytic activity of the nanoparticles was found for the largest nanoparticles (> 100 nm). It was observed that the size of the NPs is independent of the conversion efficiency of Pd²⁺, as the most catalytic active bio-Pd NPs showed the lowest conversion efficiency, with a NPs size of 39.0 nm. High removal efficiencies of these bio-Pd NPs were also found for the reductive transformation of persistent micropollutants that was present in complex matrices with environmentally relevant concentrations in 2 hr. An effect of the bio-Pd NPs on the dehalogenation of fluorinated and chlorinated pharmaceutical compounds was also proposed in this study. Another advantage of the use of bio-Pd NPs is the low mass of palladium that was used. Although palladium is expensive, high removal efficiencies are obtained in a shorter time. This study provides strong support for the use of bio-Pd NPs to efficiently remove micropollutants from the environment and the possible applicability to WWTP as a tertiary treatment system. However, before applying bio-Pd NPs in real wastewater treatment systems, more investigation is required. H₂ can be submitted by implementing an electrochemical system into the treatment plant or more research can be performed on finding an alternative electron donor for activating the catalytic activity of the bio-Pd NPs. Besides this, it is also important to recover bio-Pd NPs for economical feasibility. Recovery of Pd²⁺ from the supernatant solution, after production of bio-Pd NPs, can be achieved by the addition of *Shewanella oneidensis* to the solution, as the matrices of the cells and the supernatants are the same. It is also possible to recover leaching Pd NPs from the bio-Pd NPs, by chemical reaction, hence by the addition of nitric acid, which has been performed by other researchers. Nevertheless, more research needs to be performed on the application of bio-Pd NPs as the recovery of Pd.

Q5

Author agreement

628 The undersigned authors, with the consent of all authors,
629 hereby assign to *Journal of Environmental Sciences*, the copyright
630 in the above identified article including but not limited to the
631 right of reproduction, distribution, dissemination of informa-
632 tion networks, performance, translation, compilation, adapta-
633 tion are transferred to the editorial board of the journal world-
634 wide to be transferred, including supplemental tables, illustra-
635 tions or other information submitted in all forms and media
636 throughout the world, in all languages and format, effective
637 when and if the article is accepted for publication. The trans-
638 fer fee is free.

639 Authors also agree to the following terms:

- 640 A The article submitted is not subject to any prior claim or
641 agreement and is not under consideration for publication
642 elsewhere.
- 643 B The article contains no libelous or other unlawful state-
644 ments and does not contain any materials that violate pro-
645 prietary right of any other person, company, organization,
646 and nation.
- 647 C If the article was prepared jointly with other authors, the
648 author(s) agree with the authorship sequence.

Declaration of Competing Interest

649 The authors declare that they have no known competing fi-
650 nancial interests or personal relationships that could have ap-
651 peared to influence the work reported in this article.

Acknowledgments

652 This project has received funding from European Union's
653 Horizon 2020 research and innovation program under grant
654 agreement No. 826244. Eduardo Bolea-Fernandez thanks FWO-
655 Vlaanderen for his postdoctoral grant (12ZA320N). The au-
656 thors would like to thank Victor Lobanov, Mingsheng Jia, and
657 Hira Khan for critically reading the manuscript.

Supplementary materials

658 Supplementary material associated with this article can be
659 found, in the online version, at doi:10.1016/j.jes.2022.08.018.

REFERENCE

- 660 Abtahi, S.M., Ilyas, S., Joannis Cassan, C., Albasi, C., de Vos, W.M.,
661 2018. Micropollutants removal from secondary-treated
662 municipal wastewater using weak polyelectrolyte multilayer
663 based nanofiltration membranes. *J. Membr. Sci.* 548, 654–666.
- 664 Adams, C.P., Walker, K.A., Obare, S.O., Docherty, K.M., 2014.
665 Size-dependent antimicrobial effects of novel palladium
666 nanoparticles. *PLoS One* 9, e85981.

- Alamgholiloo, H., Pesyan, N.N., Mohammadi, R., Rostamnia, S.,
Shokouhimehr, M., 2021. Synergistic advanced oxidation
process for the fast degradation of ciprofloxacin antibiotics
using a GO/CuMOF-magnetic ternary nanocomposite. *J.*
Environ. Chem. Eng. 9, 105486. 667
668
669
Anjali, R., Shanthakumar, S., 2019. Insights on the current status
of occurrence and removal of antibiotics in wastewater by
advanced oxidation processes. *J. Environ. Manage* 246, 51–62. 670
671
672
Antonelli, R., Malpass, G.R.P., da Silva, M.G.C., Vieira, M.G.A., 2020.
Adsorption of ciprofloxacin onto thermally modified
bentonite clay: Experimental design, characterization, and
adsorbent regeneration. *J. Environ. Chem. Eng.* 8, 104553. 673
674
675
Bartolomeu, M., Neves, M.G.P.M.S., Faustino, M.A.F., Almeida, A.,
2018. Wastewater chemical contaminants: remediation by
advanced oxidation processes. *Photochem. Photobiol. Sci.* 17,
1573–1598. 676
677
678
Bernats, M., Juhna, T., 2018. Removal of phenols-like substances
in pharmaceutical wastewater with fungal bioreactors by
adding *Trametes versicolor*. *Water Sci. Technol.* 78, 743–750. 679
680
681
Bobu, M., Yediler, A., Siminiceanu, I., Zhang, F., Schulte-Hostede, S.,
2013. Comparison of different advanced oxidation processes
for the degradation of two fluoroquinolone antibiotics in
aqueous solutions. *J. Environ. Sci. Health. Toxic/hazardous*
Substance Environ. Eng. 48, 251–262. 682
683
684
Cao, Z., Liu, X., Xu, J., Zhang, J., Yang, Y., Zhou, J., et al., 2017.
Removal of antibiotic Florfenicol by sulfide-modified
nanoscale zero-valent iron. *ES&T* 51, 11269–11277. 685
686
687
Chen, Y., Chen, Y., 2021. Difference in toxicity of Pd (II) and
mechanism of action before and after reduction by *Bacillus*
wiedmannii MSM. *Environ. Sci. Pollut. Res.* 29, 1824–1835. 688
689
690
Chin, C.-J.M., Chen, T.-Y., Lee, M., Chang, C.-F., Liu, Y.-T., Kuo, Y.-T.,
2014. Effective anodic oxidation of naproxen by platinum
nanoparticles coated FTO glass. *J. Hazard. Mater.* 277, 110–119. 691
692
693
de Andrade, J.R., Oliveira, M.F., da Silva, M.G.C., Vieira, M.G.A.,
2018. Adsorption of pharmaceuticals from water and
wastewater using nonconventional low-cost materials: a
review. *Ind. Eng. Chem. Res.* 57, 3103–3127. 694
695
696
De Corte, S., Sabbe, T., Hennebel, T., Vanhaecke, L., De Gussemme, B.,
Verstraete, W., Boon, N., 2012. Doping of biogenic Pd catalysts
with Au enables dechlorination of diclofenac at
environmental conditions. *Water Res.* 46, 2718–2726. 697
698
699
De Gussemme, B., Soetaert, M., Hennebel, T., Vanhaecke, L., Boon, N.,
Verstraete, W., 2012. Catalytic dechlorination of diclofenac by
biogenic palladium in a microbial electrolysis cell. *Microb.*
Biotechnol. 5, 396–402. 700
701
702
de Santiago-Martín, A., Meffe, R., Teijón, G., Martínez
Hernández, V., López-Heras, I., Alonso Alonso, C., et al., 2020.
Pharmaceuticals and trace metals in the surface water used
for crop irrigation: risk to health or natural attenuation? *Sci.*
Total Environ. 705, 135825. 703
704
705
De Windt, W., Boon, N., Van den Bulcke, J., Rubberecht, L., Prata, F.,
Mast, J., et al., 2006. Biological control of the size and reactivity
of catalytic Pd(0) produced by *Shewanella oneidensis*. *Antonie*
Van Leeuwenhoek 90, 377–389. 706
707
708
Deplanche, K., Bennett, J.A., Mikheenko, I.P., Omajali, J., Wells, A.S.,
Meadows, R.E., et al., 2014. Catalytic activity of
biomass-supported Pd nanoparticles: Influence of the
biological component in catalytic efficacy and potential
application in 'green' synthesis of fine chemicals and
pharmaceuticals. *Appl. Catal.* 147, 651–665. 709
710
711
Dundas, C.M., Graham, A.J., Romanovicz, D.K., Keitz, B.K., 2018.
Extracellular electron transfer by *shewanella oneidensis*
controls palladium nanoparticle phenotype. *ACS Synth. Biol.*
7, 2726–2736. 712
713
714
Ershov, B.G., Solovov, R.D., Abkhalimov, E.V., 2014. Palladium
nanoparticles in aqueous solution: Preparation, properties,
and effect of their size on catalytic activity. *Colloid J.* 76,
553–557. 715
716
717
718
719
720
721
722
723
724
725
726
727
728
729
730
731
732
733
734

- 735 Forrez, I., Carballa, M., Fink, G., Wick, A., Hennebel, T.,
736 Vanhaecke, L., et al., 2011. Biogenic metals for the oxidative
737 and reductive removal of pharmaceuticals, biocides and
738 iodinated contrast media in a polishing membrane bioreactor.
739 *Water Res.* 45, 1763–1773.
- 740 Freitas, N.S., Alzamora, M., Sánchez, D.R., Licea, Y.E., Senra, J.D.,
741 Carvalho, N.M.F., 2021. Green palladium nanoparticles
742 prepared with glycerol and supported on maghemite for dye
743 removal application. *J. Environ. Chem. Eng.* 9, 104856.
- 744 Gautam, P.K., Singh, A., Misra, K., Sahoo, A.K., Samanta, S.K., 2019.
745 Synthesis and applications of biogenic nanomaterials in
746 drinking and wastewater treatment. *Environ. Manage.* 231,
747 734–748.
- 748 Gomez-Bolivar, J., Mikheenko, I.P., Orozco, R.L., Sharma, S.,
749 Banerjee, D., Walker, M., et al., 2019. Synthesis of Pd/Ru
750 bimetallic nanoparticles by *Escherichia coli* and potential as a
751 catalyst for upgrading 5-Hydroxymethyl furfural into liquid
752 fuel precursors. *Front. Microbiol.* 1276.
- 753 Han, J., Hu, W., Deng, H., 2009. Adsorption of hydrogen on
754 palladium nanoparticle surfaces. *Surf. Interface Anal.* 41,
755 590–594.
- 756 Hazarika, M., Borah, D., Bora, P., Silva, A.R., Das, P., 2017. Biogenic
757 synthesis of palladium nanoparticles and their applications
758 as catalyst and antimicrobial agent. *PLoS One* 12, e0184936.
- 759 He, P., Mao, T., Wang, A., Yin, Y., Shen, J., Chen, H., Zhang, P., 2020.
760 Enhanced reductive removal of ciprofloxacin in
761 pharmaceutical wastewater using biogenic palladium
762 nanoparticles by bubbling H₂. *RSC Adv.* 10, 26067–26077.
- 763 Hennebel, T., Benner, J., Clauwaert, P., Vanhaecke, L., Aelterman, P.,
764 Callebaut, R., et al., 2011. Dehalogenation of environmental
765 pollutants in microbial electrolysis cells with biogenic
766 palladium nanoparticles. *Biotechnol. Lett.* 33, 89–95.
- 767 Hou, Y.-N., Zhang, B., Yun, H., Yang, Z.-N., Han, J.-L., Zhou, J., et al.,
768 2017. Palladized cells as suspension catalyst and
769 electrochemical catalyst for reductively degrading aromatics
770 contaminants: Roles of Pd size and distribution. *Water Res.*
771 125, 288–297.
- 772 Jiang, W.-L., Ding, Y.-C., Haider, M.R., Han, J.-L., Liang, B., Xia, X.,
773 et al., 2020. A novel TiO₂/graphite felt photoanode assisted
774 electro-Fenton catalytic membrane process for sequential
775 degradation of antibiotic florfenicol and elimination of its
776 antibacterial activity. *Chem. Eng. J.* 391, 123503.
- 777 Khataee, A.R., Kasiri, M.B., 2010. Photocatalytic degradation of
778 organic dyes in the presence of nanostructured titanium
779 dioxide: Influence of the chemical structure of dyes. *J. Mol.*
780 *Catal. A Chem.* 328, 8–26.
- 781 Kluson, P., Cerveny, L., 1995. Selective hydrogenation over
782 ruthenium catalysts. *Appl. Catal.* 128, 13–31.
- 783 Liu, H., Han, J., Yuan, J., Liu, C., Wang, D., Liu, T., et al., 2019. Deep
784 dehalogenation of Florfenicol Using Crystalline CoP
785 Nanosheet Arrays on a Ti Plate via direct cathodic reduction
786 and atomic H. *ES&T* 53, 11932–11940.
- 787 Long, M., Donoso, J., Bhati, M., Elias, W.C., Heck, K.N., Luo, Y.-H.,
788 et al., 2021. Adsorption and reductive defluorination of
789 perfluorooctanoic acid over palladium nanoparticles. *ES&T* 55,
790 14836–14843.
- 791 Lovley, D.R., 1993. Dissimilatory metal reduction. *Ann. Rev.*
792 *Microbiol.* 47, 263–290.
- 793 Martins, M., Mourato, C., Sanches, S., Noronha, J.P., Crespo, M.T.B.,
794 Pereira, I.A.C., 2017. Biogenic platinum and palladium
795 nanoparticles as new catalysts for the removal of
796 pharmaceutical compounds. *Water Res.* 108, 160–168.
- 797 Miao, D., Peng, J., Wang, M., Shao, S., Wang, L., Gao, S., 2018.
798 Removal of atorvastatin in water mediated by CuFe₂O₄
799 activated peroxymonosulfate. *Chem. Eng. J.* 346, 1–10.
- 800 Nguyen, C.H., Fu, C.-C., Juang, R.-S., 2018. Degradation of
801 methylene blue and methyl orange by palladium-doped TiO₂
photocatalysis for water reuse: Efficiency and degradation
pathways. *J. Clean. Prod.* 202, 413–427.
- Olvera-Vargas, H., Oturan, N., Buisson, D., van Hullebusch, E.D.,
Oturan, M.A., 2015. Electro-oxidation of the pharmaceutical
furosemide: kinetics, mechanism, and By-Products. *clean.* 43,
1455–1463 Wein.
- Omajali, J.B., Gomez-Bolivar, J., Mikheenko, I.P., Sharma, S.,
Kayode, B., Al-Duri, B., et al., 2019. Novel catalytically active
Pd/Ru bimetallic nanoparticles synthesized by *Bacillus*
benzeovorans. *Sci. Rep.* 9, 4715.
- Osawa, R.A., Carvalho, A.P., Monteiro, O.C., Oliveira, M.C.,
Florêncio, M.H., 2019. Transformation products of citalopram:
Identification, wastewater analysis and in silico toxicological
assessment. *Chemosphere* 217, 858–868.
- Pandey, A., Shukla, P., Srivastava, P., 2020. Remediation of dyes in
water using green synthesized nanoparticles (NPs). *IJPE* 6,
68–84.
- Peñacobá-Antona, L., Senán-Salinas, J., Aguirre-Sierra, A.,
Letón, P., Salas, J.J., García-Calvo, E., Esteve-Núñez, A., 2021.
Assessing METland@ design and performance through LCA:
techno-environmental study with multifunctional unit
perspective. *Front. Microbiol.* 12, 652173.
- Quan, X., Zhang, X., Sun, Y., Zhao, J., 2018. Iohexol degradation by
biogenic palladium nanoparticles hosted in anaerobic
granular sludge. *Front. Microbiol.* 9, 1980.
- Rotaru, A.-E., Jiang, W., Finster, K., Skrydstrup, T., Meyer, R.L., 2012.
Non-enzymatic palladium recovery on microbial and
synthetic surfaces. *Biotechnol. Bioeng.* 109, 1889–1897.
- Saldan, I., Semenyuk, Y., Marchuk, I., Reshetnyak, O., 2015.
Chemical synthesis and application of palladium
nanoparticles. *J. Mater. Sci.* 50, 2337–2354.
- Sivamaruthi, B.S., Ramkumar, V.S., Archunan, G., Chaiyasut, C.,
Suganthi, N., 2019. Biogenic synthesis of silver palladium
bimetallic nanoparticles from fruit extract of *Terminalia*
chebula – In vitro evaluation of anticancer and antimicrobial
activity. *J. Drug Deliv Sci Technol* 51, 139–151.
- Tuo, Y., Liu, G., Dong, B., Yu, H., Zhou, J., Wang, J., Jin, R., 2017.
Microbial synthesis of bimetallic PdPt nanoparticles for
catalytic reduction of 4-nitrophenol. *Environ. Sci. Pollut. Res.*
24, 5249–5258.
- Wang, P.-t., Song, Y.-h., Fan, H.-c., Yu, L., 2018. Bioreduction of azo
dyes was enhanced by in-situ biogenic palladium
nanoparticles. *Bioresour. Technol.* 266, 176–180.
- Xiong, L., Zhang, X., Huang, Y.-X., Liu, W.-J., Chen, Y.-L., Yu, S.-S.,
et al., 2018. Biogenic synthesis of Pd-Based nanoparticles with
enhanced catalytic activity. *ACS Appl. Nano Mater.* 1,
1467–1475.
- Xu, H., Tan, L., Cui, H., Xu, M., Xiao, Y., Wu, H., et al., 2018.
Characterization of Pd(II) biosorption in aqueous solution by
Shewanella oneidensis MR-1. *J. Mol. Liq.* 255, 333–340.
- Yagub, M.T., Sen, T.K., Afroz, S., Ang, H.M., 2014. Dye and its
removal from aqueous solution by adsorption: a review. *Adv.*
Colloid Interface Sci. 209, 172–184.
- Yang, Z.-N., Hou, Y.-N., Zhang, B., Cheng, H.-Y., Yong, Y.-C.,
Liu, W.-Z., et al., 2020. Insights into palladium nanoparticles
produced by *Shewanella oneidensis* MR-1: Roles of NADH
dehydrogenases and hydrogenases. *Environ. Res.* 191, 110196.
- Yudanov, I.V., Genest, A., Rösch, N., 2011. DFT studies of palladium
model catalysts: structure and size effects. *J. Clust. Sci.* 22,
433–448.
- Yudanov, I.V., Sahnoun, R., Neyman, K.M., Rösch, N., Hoffmann, J.,
Schauermann, S., et al., 2003. CO adsorption on Pd
nanoparticles: density functional and vibrational
spectroscopy studies. *J. Phys. Chem. B* 107, 255–264.
- Zhang, M., Song, Q., He, Z., Wang, Q., Wang, L., Zhang, X., Li, G.,
2022. Tuning the mesopore-acid-metal balance in Pd/HY for
efficient deep hydrogenation saturation of naphthalene. *Int. J.*
Hydrog. Energy 47, 20881–20893.